Influence of Rhenium and Ruthenium on the Local Mechanical Properties of the γ and γ' Phase in Nickel-Base Superalloys

Steffen Neumeier, Florian Pyczak, Mathias Göken

Influence of Rhenium and Ruthenium on the Local Mechanical Properties of the γ and γ' Phase in Nickel-Base Superalloys

Journal:	*Philosophical Magazine & Philosophical Magazine Letters*
Manuscript ID:	TPHM-10-Oct-0468.R1
Journal Selection:	Philosophical Magazine
Date Submitted by the Author:	20-Apr-2011
Complete List of Authors:	Neumeier, Steffen; University Erlangen-Nürnberg, Materials Science and Engineering Pyczak, Florian; GKSS Research Centre Geesthacht, Institute for Materials Research Göken, Mathias; University Erlangen-Nürnberg, Materials Science and Engineering
Keywords:	nanoindentation, atomic force microscopy, rhenium, Ni-based superalloys
Keywords (user supplied):	ruthenium, solid solution hardening, partitioning behaviour

Influence of Rhenium and Ruthenium on the Local Mechanical Properties of the γ and γ′ Phase in Nickel-Base Superalloys

S. Neumeier[1*], F. Pyczak[1,2], M. Göken[1]

[1]*Department of Materials Science & Engineering, Institute I, University Erlangen-Nürnberg, Erlangen, Germany*
[2]*now at: Institute for Materials Research, HZG Research Centre Geesthacht, Geesthacht, Germany*

[*]Corresponding author.
Department of Materials Science and Engineering, University Erlangen-Nürnberg, Martensstrasse 5, 91058 Erlangen, Germany, E-mail address: steffen.neumeier@ww.uni-erlangen.de

Abstract

The effect of rhenium and ruthenium on the hardness of the γ' precipitates and the γ matrix in nickel-base superalloys was investigated using a nanoindenting atomic force microscope. The partitioning behaviour of the alloying elements and the lattice misfit between the γ and γ' phase were determined in fully homogenised samples to explain the alloying effects. Rhenium strongly strengthens γ as it predominantly partitions to γ and has a strong solid solution hardening effect. Ruthenium strengthens both γ and γ' due to a more homogeneous partitioning behaviour. Ruthenium was found to cause less partitioning of Rhenium to γ. This results in a stronger increase of the γ' hardness. The change of the nanoindentation-derived hardness of both phases could be mainly attributed to the solid solution strengthening of Re and Ru.

Keywords: Nanoindentation, Atomic force microscopy, Rhenium, Ruthenium, Solid solution hardening, Partitioning behaviour

1. Introduction

Turbine blades in gas turbines are manufactured of nickel-base superalloys which possess excellent mechanical properties at high temperatures due to the γ/γ′ microstructure. The face centred cubic γ matrix phase is strengthened by the intermetallic γ′ precipitate phase ($L1_2$ crystal structure), which is coherently embedded in the γ matrix. Nickel-base superalloys are alloyed with an increasing amount of refractory elements to improve their temperature capability and creep resistance. Amongst more than ten alloying elements Re plays a key role in promoting creep resistance. Re itself partitions predominantly to the γ matrix [1-5] and acts accordingly as a strong solid solution hardening element of this phase [6-8]. In recent years Ru has been alloyed to nickel-base superalloys to prevent the formation of deleterious topologically close-packed (TCP) phases [9, 10].
In the present study the solid solution hardening effect of Re and Ru in nickel-base superalloys was investigated by nanoindenting atomic force microscopy (NI-AFM) to characterise to which extent Ru acts as a solid solution hardener. Additionally, it is of special

interest to relate these investigations on the effects of Re and Ru on the local hardness of the phases γ and γ′ with investigations of the γ/γ′ partitioning behaviour of these elements in the different alloys.

It was reported by O'Hara et al. that Re is less strongly enriched in the γ phase if Ru is added [11]. This so-called reverse partitioning effect is highly debated as it could be found in some alloys [12-14] while it was absent in others [1, 15]. If reverse partitioning occurs it should have an influence on the hardness of the γ and γ′ phase in alloys with different contents of Re and Ru as were investigated in this study. To relate the hardness with the partitioning behaviour of the alloying elements at room temperature, the concentration of the elements in the γ and γ' phase was measured by energy dispersive spectroscopy (EDS) in a transmission electron microscope (TEM).

While alloying elements can influence the hardness directly by solid solution hardening also indirect effects of an alloying element on the mechanical properties by changing the γ-channel width or altering the lattice misfit inducing different coherency stresses in matrix and precipitate phase are possible. To ensure that solid solution hardening is the main contribution to hardness changes the coherency stresses and lattice misfit were characterized by X-ray diffraction and the width of the γ-channels was determined in the alloys under investigation.

2. Experimental Details

Four experimental alloys with an identical base composition possessing different amounts of Re and Ru were directionally solidified in a laboratory-scale Bridgman furnace as bars of 8 cm length and 2.4 cm diameter. The nominal alloy compositions are listed in Table 1. Samples of all alloys were solution heat treated between 1300°C and 1305°C for 48 h to generate a homogeneous element distribution without any residual Re segregation. Electron probe micro-analyser (EPMA) measurements were performed in order to verify the even distribution of the strongly segregating element Re after the solution heat treatment. The samples were subsequently annealed at 1100°C for 24h and additionally at 850°C for 24 h to obtain a coarse γ/γ'-microstructure which allows separate indentation of both phases. For AFM investigations surfaces parallel to the {001} crystallographic plane (perpendicular to solidification direction) were ground and polished with diamond suspension. Afterwards a chemo-mechanical polishing process with nanodispersive SiO_2 (OPU, Struers) was used to generate a smooth surface topography with the matrix phase elevated by a height difference of about 5-10 nm. The local roughness of each phase did not exceed 2 nm. The nanoindentation investigations were performed at room temperature with a Triboscope force transducer from Hysitron mounted on a Veeco Instruments Multimode AFM (NI-AFM). For scanning as well as indentation a three-sided pyramidal diamond tip (cube corner geometry) was used. During the indentation the currently applied load and associated indentation depth (displacement) was recorded simultaneously. The nano-hardness of γ and γ′ were calculated from the unloading part of the load-displacement curves according to the Oliver/Pharr method [16].

Alloy ReRu with the smallest precipitates among the investigated alloys exhibited an average γ' size and γ channel width of at least 790 nm and 250 nm, respectively. As an example an AFM image of Alloy Re including fields of nanoindents generated by

indentations with a maximum load P_{max} of 250 µN, 500 µN and 1000 µN, respectively are shown in Fig. **1a**. Various maximum loads were applied to obtain the optimal settings for the experiments. For further hardness measurements only a maximum indentation load of 250 µN was applied to test both phases separately (Fig. 1c-f). When applying this load a maximum depth in the range of 45 nm was obtained in the softer γ matrix. Additionally, this sample of Alloy Re which contains small secondary γ' precipitates in the γ matrix (precipitate size < 100nm) (Fig. 1b) was utilized to investigate the influence of these secondary γ' precipitates on the γ hardness. This microstructure was achieved by omitting the second heat treatment step. In the specimens investigated to study the influence of the alloying elements, secondary γ′-precipitates in the matrix channels were absent (Fig. 1c-f), which could be confirmed by TEM investigations on similar heat treated samples [14].

The nanoindentation experiments on two different microstructures with and without secondary γ' precipitates in the γ matrix of Alloy Re (microstructure: Fig.1b und 1d, indentation curves: Fig.2) show the necessity of a secondary γ' precipitate free γ matrix to obtain the true hardness of the γ phase.

The sample with secondary γ' precipitates in the γ matrix leads to a much smaller indentation depth and a much higher hardness, respectively, of the γ phase with 6.56 GPa compared to 6.06 GPa of the secondary γ' precipitate free sample, while the hardness of the γ' phase in both samples is almost indentical with 8.47 GPa and 8.62 GPa, respectively.

For the investigation of the influence of Re and Ru on the solid solution hardening at least 10 indents for each phase were evaluated. In order to ensure that all evaluated indents where wholly contained within the precipitate or the matrix phase, respectively, the load-displacement curves were analysed carefully. In case of the indentation of one γ' precipitate with a subsequent penetration of a subjacent γ matrix channel the load displacement curve initially **resembles** the behaviour for an indentation in the precipitate phase. At higher indentation depths a transition to the indentation behaviour of the softer matrix phase is observed. This leads to a significantly increased final indentation depth. In case of an initial indentation of the γ matrix with a subsequent penetration of a γ' precipitate the load-displacement curve shows initially a similar behaviour to a load-displacement curve of pure γ, but deviates from it during the ongoing indentation. In comparison to other load-displacement curves, derived from the indentation of γ' precipitates or the γ matrix, load displacement curves showing this transition behaviour were clearly distinguishable (see Fig. 3). Finite element simulations explained this experimentally observed transition from precipitate to matrix deformation (and vice versa) and should be excluded from the analysis [17]. Accordingly such load-displacement curves have not been evaluated.

In addition to the NI-AFM **investigations,** X-ray diffraction experiments were performed at room temperature on the different alloys by using a high resolution double crystal X-ray diffractometer with **monochromated** copper $K_{\alpha 1}$ X-rays. Further details of the set-up can be found in [18]. These experiments were conducted to examine the influence of the coherency stresses which might also contribute to the measured hardness. Internal coherency stresses occur in nickel-base superalloys due to a lattice misfit δ between the γ and γ′ phase. As the lattice parameters of both phases γ and γ′ are quite similar in nickel base superalloys, the (002) peaks of both phases overlap with each other. Therefore the detected (002) peak was deconvoluted into subpeaks to obtain the lattice parameter of γ and γ′ by fitting the measured (002) peak with **Pseudo-Voigtfunctions**, which are a combination of a Gaussian and a Lorentzian function [19]. The constrained lattice misfit δ of the alloys under investigation

was derived from the lattice parameter a_γ and $a_{\gamma'}$ of the γ and γ′ phase using the following formula:

$$\delta = \frac{2\left(a_{\gamma'} - a_\gamma\right)}{a_{\gamma'} + a_\gamma} \quad \textbf{(1)}$$

The specimens for the TEM investigations were annealed at 1100°C for 4h and at 850°C for 24h after the solution heat treatment. Thin slices were cut from the specimens, ground to a thickness of about 70 µm and subsequently electrochemically thinned by using an agent of ethanol and perchloric acid. For measuring the local chemical composition in the γ and γ′ phase, a Philips CM200 TEM with an EDAX EDS system operating at 200 kV was used. The EDX spectra were evaluated using the MThin method integrated in the EDAX software. **Elsewhere, we have presented the partitioning behaviour of the alloying elements as a function of temperature** [20].

3. Results and Discussion

3.1 Segregation:

Electron probe micro-analyser (EPMA) measurements were performed in order to verify the even distribution after the solution heat treatment of the strongly segregating element Re. In the as-cast state the Re-containing alloys Alloy Re and Alloy ReRu possess an average primary dendrite arm spacing between 225 µm and 255µm and a segregation coefficient k_{Re}^{Seg} of 3.43 and 3.23, respectively. k_{Re}^{Seg} is the ratio of the concentration of Re in the dendrite core to the interdendritic area (Fig. **4a**). Due to the long annealing times of 48hrs **used** at 1300 °C for Alloy Re and 1305 °C for Alloy ReRu, a fully homogeneous element distribution could be achieved (k_{Re}^{Seg} = 1, see Fig. **4** b), which is essential for nanoindentation experiments.

3.2 Hardness:

The hardness of the γ and γ' phase in the investigated experimental alloys which possess no secondary γ' precipitates are shown in Fig. **5**. These results were used to study the solid solution hardening of the alloying elements Re and Ru.

The measured γ and γ' hardness values in the Re-free variant Alloy 0 are 5.57 GPa and 8.46 GPa , respectively which are in good agreement with the hardness values obtained in previous studies [6, 21]. Early works about nanoindentation measurements of the phases γ and γ' in the Nickel-base superalloy CMSX-6 have already shown that the γ' precipitates are much harder than the γ matrix [6, 21]. When comparing Alloy 0 to Alloy Re a strong increase in the hardness of the γ matrix phase is noted whereas the hardness of the γ' precipitate phase stays more or less constant.

This can be attributed to the 3 wt % (0.9 at. %) Re which are added in Alloy Re. These results again correspond with what is reported by Durst et al. for the second generation nickel-base superalloy CMSX-4 which contains also 3 wt.% Re [6]. An addition of 3 wt % (1.7 at. %) Ru to the base Alloy 0 results in an increase of the hardness of both phases γ and

γ′ in Alloy Ru. The Nickel-base superalloy Alloy ReRu with 3 wt % Re and 3 wt % Ru has the highest hardness of the γ' phase of all alloys in this study and a hardness of the γ matrix phase similar to Alloy Re and Alloy Ru.

3.3 Partitioning behaviour:

To understand the change of hardness of the respective phases in the different alloys the partitioning behaviour of the alloying elements Re and Ru has to be considered. The partitioning behavior of the alloying elements by means of the partitioning coefficient *k* is shown in Fig. 6. The partition coefficient *k* is defined as $k = c_i^{\gamma'}/c_i^{\gamma}$ where $c_i^{\gamma'}$ and c_i^{γ} are the concentrations of an alloying element *i* in the phases γ′ and γ, respectively. Elements with an value $k < 1$ (Re, Cr, Co, Ru and Mo) partition preferentially to the γ matrix while a *k* value greater than 1 indicates preferred partitioning to the γ' precipitates (Al and Ti). *k*-values for Ta were not evaluated as the overall low concentration of Ta in the γ matrix caused errors for the *k*-values of this element **would be even greater than the *k*-values themselves**. It is noted that reverse partitioning of Re and to a lesser extent Mo in the presence of Ru is found for Alloy ReRu in this work. A further study on these experimental alloys also reveals that this influence of Ru on the partitioning behaviour is also present at high temperatures [20].
All differences in the hardness values measured by nanoindentation in this work can be understood qualitatively from the partitioning behaviour of the alloying elements**, as follows**. Since Re partitions predominantly to the γ matrix (Fig. 6) and Re is known to be a strong solid solution hardener, Re mainly increases the hardness of the γ matrix phase as observed in Alloy Re.
On the other hand the partitioning of Ru to the γ matrix is not as pronounced compared to Re. Therefore a certain amount of Ru is also present in the γ' precipitates. Hence, Ru increases the hardness of both phases γ and γ′ as found when comparing Alloy Ru with Alloy 0. This is in good agreement with the work of Yeh et al [8]. They investigated single phase γ and γ' alloys and found that Ru increases the flow stresses of both phases at elevated temperatures [8]. The fact that the hardness of the γ matrix in Alloy Re and Alloy Ru is almost identical originates to some degree from a rather similar atomic concentration of Ru in the γ phase in Alloy Ru compared with Re in the γ phase in Alloy Re (c_{Ru}^{γ} =2.94 at % and c_{Re}^{γ} =3.81 at %, respectively), even though Ru partitions less to γ than Re. This is due to the fact that when comparing atomic concentrations a higher total amount of Ru is alloyed in Alloy Ru than Re in Alloy Re. Another reason might be the influence of Re and Ru on the partitioning behaviour of the other alloying elements.
When comparing the results from nanoindentation measurements of Alloy Ru and Alloy Re with Alloy ReRu the reverse partitioning of Re and Mo in Alloy ReRu has to be considered to explain the hardness of the γ' phase. Not only the addition of Ru to Alloy Re increases the concentration of solid solution hardening elements in the γ' phase of Alloy ReRu, but also the fact that Re and Mo partitions more homogeneously between γ and γ' in presence of Ru (see Fig. 6). Accordingly the overall concentration of the solid solution hardening elements Re, Mo and Ru increases strongly in the γ' precipitates from $c_{(Mo+Re+Ru)}^{\gamma'}$ = 2.27 at.% in Alloy Re to $c_{(Mo+Re+Ru)}^{\gamma'}$ = 5.35 at.% in Alloy ReRu. Consequently, the hardness of γ' increases more strongly in Alloy ReRu even though Ru partitions to the γ matrix. Additionally the stronger increase of the γ' hardness from Alloy Ru to Alloy ReRu compared

to the increase between Alloy 0 and Alloy Re confirms, that the concentration of Re in the γ' phase of Alloy ReRu is higher than in Alloy Re.

3.4 Lattice misfit:

While up to now the effect of the alloying elements Re and Ru on the mechanical properties of the γ and γ′ phase was interpreted as a result of solid solution hardening there exists another possibility. Coherency stresses due to the lattice misfit at the γ/γ' interface may also have an influence on the local hardness. To make sure that solid solution hardening and not coherency stress is the dominant effect by which Re and Ru influence the mechanical properties in the alloys under investigation the lattice misfit of the alloys was investigated by means of XRD. In Fig. 7 the (002) X-ray peaks of Alloy 0 and Alloy Ru are shown.
Alloy 0 possess a much larger and positive lattice misfit δ of about +0.1% in comparison to Alloy Ru which has a slightly negative lattice misfit close to 0 at room temperature. The fact that the absolute value of the lattice misfit of Alloy 0, for example, is greater than the absolute value of the lattice misfit of Alloy Ru but the hardness of the γ matrix in Alloy Ru is much bigger than in Alloy 0 implies that the direct effect of solid solution strengthening due to the different chemical composition on the nanoindentation-derived hardness at room temperature is much stronger than the indirect effect of the coherency stresses due to the changed chemical composition. Because the higher the amount of lattice misfit the higher the resulting coherency stresses should be (assuming similar elastic properties for phases γ and γ′ in the alloys). That the coherency stresses do not significantly influence the hardness measurements can be explained with the relatively coarse microstructure and the choice of the indentation site. In order to measure the influence of the alloying elements on the solid solution strengthening of the γ and γ′ phase the γ matrix channel crosses and the interior of the γ' precipitates were indented (see Fig.1). Müller et al. have shown in their work about modelling of misfit stresses in nickel-base superalloys that the interior of the precipitates is on a low stress level and that the stresses in the γ channels are much higher than in the γ channel crosses, which are nearly stress free [22]. Consequently, it is assumed that the misfit stresses do not significantly affect the relative change of the nanoindentation-derived hardness. Accordingly, the differences in hardness in the investigated alloys can be related mainly to the solid solutioning effect of the alloying elements. **This coincides with** a similar study on the Nickel-base superalloys CMSX-4 and CMSX-10. Durst et al. have shown that the hardening effect of an alloying element **on the γ and γ′ phase** is similar in samples **with coherently embedded γ′ precipitates and therefore with internal coherency stresses** compared to long term heat treated stress-relieved samples **with semicoherent γ′ precipitates** [6].

3.5 Influence of solid solution strengthening on hardness:

To relate the hardness values measured by nanoindentation quantitatively to the changes in chemical composition of the phases γ and γ′ it is necessary to judge the influence of an alloying element on the hardness of the respective phase. As mentioned before, it is reasonable to assume that the strengthening effect of the alloying elements in nickel-base superalloys measured here by nanoindentation is due to solid solution strengthening. Solid solution strengthening is an effect of an atomic diameter mismatch between the alloying

element and the surrounding host atoms and a local modification of the shear modulus due to the presence of the alloying element, i.e. the paraelastic and dielastic interaction [23]. The fact, that the alloying elements change the lattice parameter of the γ and γ' phase in the alloys under investigation could be already confirmed by XRD measurements in a previous work of the authors [14].

In principle the strengthening effect of the solid solution hardeners in the γ matrix and γ' precipitates can be calculated by the method of Gypen and Deruyttere [24]:

$$\Delta\sigma = \left(\sum_i k_i^{\frac{1}{n}} c_i \right)^n \quad (2)$$

where $\Delta\sigma$ is the increase of the plastic flow stress at 77 K due to alloying in pure nickel and pure Ni_3Al, respectively, the constant n is taken to be ½ while c_i is the concentration and k_i the strengthening constant of the solute i.

For the γ matrix the values k for all alloying elements contained in the four alloys under investigation here were determined by Roth et al. [25] and Diologent et al. [26]. The strengthening constants k_i^{γ} for the alloying elements Re, Ru and Mo in the γ matrix for example are 1000 MPa/$\sqrt{at.\,fraction}$, 1068 MPa/$\sqrt{at.\,fraction}$ and 1015 MPa/$\sqrt{at.\,fraction}$, respectively. It is interesting to note that the elements Ru and Mo have a similar strengthening effect per $\sqrt{at.\,fraction}$ as Re. Therefore it is understandable that significant increases in hardness can also be achieved by addition of Ru in the absence of Re as was observed in Alloy Ru. Thus, the large strengthening effect of Re additions frequently reported in literature [6-8] is not caused by an extraordinary solid solution strengthening of Re per atom compared with other refractory elements as Ru or Mo. It is most probably mainly due to the pronounced enrichment of Re in the γ matrix where plastic deformation in nickel-base superalloys takes mainly place. To calculate $\Delta\sigma$, only the refractory elements Re, Mo and Ru were chosen since they differ significantly in concentration within the respective phase in the four experimental alloys. As presented in Fig 6, the TEM-EDS results show that these elements influence the magnitude of the partitioning behaviour of the respective other element. Accordingly, due to this interaction the change of the hardness cannot be attributed to just one alloying element alone but the overall change of the chemical composition in γ and γ' has to be examined. The resulting increase of yield stress $\Delta\sigma$ in the γ matrix due to the solid solution strengtheners Re, Ru and Mo, derived from the method of Gypen and Deruyttere, are 207 MPa in Alloy 0, 307 MPa in Alloy Re, 255 MPa in Alloy Ru and 356 MPa in Alloy ReRu. The calculated increase of the plastic flow stress between Alloy 0 and Alloy Re, Alloy Ru and Alloy ReRu are in good agreement with the hardness differences of the γ matrix measured by nano-indentation in the AFM. Only the measured hardness of the γ matrix of Alloy Ru seems too high compared to the calculations. The reason might be the usage of another cube corner tip in the case of Alloy Ru. Although the indentation tips were calibrated carefully, a slight difference in the measured hardness cannot be excluded. A further reason for slight differences between the estimated increase of yield stress $\Delta\sigma$ in the γ matrix of the four alloys and the corresponding hardness might be the fact that the content of other solid solution strengthening elements like Ti and Ta varies also slightly between the different alloys which affects the hardness of both phases. **The resulting differences in *k*-values (e.g. up to 28% for Ti within the four alloys) due to the variation in concentration of the elements in the γ and γ′ phase is shown in Fig. 6.**

To calculate to increase of yield stress $\Delta\sigma$ in the γ' phase the strengthening constants $k_i^{\gamma'}$ for the alloying elements in pure Ni_3Al are needed. Unfortunately, not all strengthening

constants $k_i^{\gamma'}$ are available in literature for the elements under investigation here. While Mishima et al. have determined the influence of the solute concentration on the 0.2% flow stress in Ni_3Al at 77 K for a number of elements including Mo [27] no values for Re and Ru are available in their work or elsewhere.

Thus it is not possible to calculate the increase of the yield stress $\Delta\sigma$ in both phases γ and γ′ due to the lack of strengthening constants $k_i^{\gamma'}$ for the γ′ phase. Nevertheless, one could qualitatively illustrate the correspondence between the changes in the content of solid solution hardening elements and hardness measured by nanoindentation. This is shown in Fig. 8 where the hardness in the phases γ and γ′ is plotted over the **square root of the** sum of atomic concentrations of Mo, Ru and Re in the respective phase of the different alloys.

Obviously for the γ matrix as well as for the γ′ precipitate phase the hardness shows a dependence of the square root of sum of concentrations of Mo, Ru and Re. This behaviour is expected from the formula of Gypen and Deruyttere for solid solution hardening. Consequently, not only in the γ matrix but also in the γ′ phase solid solution hardening can explain the increase in hardness as effect of alloying additions. It is not surprising that under consideration of the measurement errors all points for the γ phase fall on one line. While no strengthening constants for the different alloying elements were considered the strengthening constants k_i^{γ} for the elements Mo, Ru and Re in γ as was already mentioned above are almost equal. Accordingly to omit them does not change the plot in Fig. 8 qualitatively. It is interesting to note that also the hardness values for the γ′ precipitates fall on one line. This is a hint that the strengthening effects of Mo, Ru and Re in the γ′ phase are also similar.

In summary, the main observation is that the increase of the local hardness in both phases γ and γ′ is an effect of solid solution strengthening of Re, Ru and Mo in the respective phase.

4. Conclusions:

The following conclusions can be drawn from this work.

1) Re acts mainly as a potent solid solution hardener in the γ matrix due to its pronounced tendency to partition to the γ phase.
2) Ru itself strengthens both phases γ and γ' due to a weaker partitioning preference for the γ matrix compared with Re.
3) Ru causes less partitioning of Re and Mo to the γ matrix which results in a stronger increase of the hardness of the γ' phase than explainable by the amount of Ru partitioning to γ′ alone.
4) The changes of the hardness of the phases γ and γ′ can be explained quantitatively by the solid solution strengthening of the alloying elements Re, Ru and Mo.

Acknowledgements:

The authors gratefully acknowledge the German Research Foundation (DFG) for funding of this work in the framework of the Research Training Group 1229/1 “Stable and Metastable Multiphase Systems for High Temperature Applications”

References:

[1] A. Volek, F. Pyczak, R.F. Singer and H. Mughrabi, Scripta Mat. 52 (2005) p.141.

[2] F. Pyczak, B. Devrient and H. Mughrabi, Superalloys 2004, eds. K.A. Green et al., The Minerals, Metals and Materials Society, Warrendale, PA, 2004, p.827.

[3] L.J. Carroll, Q. Feng, J.F. Mansfield and T.M. Pollock, Mat. Sc. Engin. A 457 (2007) p.292.

[4] H. Murakami, T. Honma, Y. Koizumi and H. Harada, Superalloys 2000, eds. T.M. Pollock et al., The Minerals, Metals and Materials Society, Warrendale, PA, 2000, p.747.

[5] R.C. Reed, A.C. Yeh, S. Tin, S.S. Babu and M.K. Miller, Scripta Mat. 51 (2004) p.327.

[6] K. Durst and M. Göken, Mat. Sc. Engin. A 387-389 (2004) p.312.

[7] A.F. Giamei and D.L. Anton, Metall. Trans. 16A (1985) p.1997.

[8] A.C. Yeh and S. Tin, Scripta Mat. 52 (2005) p.519.

[9] A.C Yeh, C.M.F Rae and S Tin, Superalloys 2004, eds. K.A. Green et al., The Minerals, Metals and Materials Society, Warrendale, PA, 2004, p.677.

[10] A. Sato, H. Harada, T. Yokokawa, T. Murakumo, Y. Koizumi, T Kobayashi and H. Imai, Scripta Mat. 54 (2006) p.1679.

[11] K.S. O'Hara, W.S. Walston, E.W. Ross and R. Darolia, US Patent No. 5,482,789, General Electric Company (1996).

[12] A.P. Ofori, C.J. Humphreys, S. Tin and C.N. Jones, Superalloys 2004, eds. K.A. Green et al., The Minerals, Metals and Materials Society, Warrendale, PA, 2004, p.787.

[13] Y. Han, W. Ma, Z. Dong, S. Li and S. Gong, Superalloys 2008, eds. R.C. Reed et al., The Minerals, Metals and Materials Society, Warrendale, PA, 2008, p.91.

[14] S. Neumeier, F. Pyczak and M. Göken, Superalloys 2008, eds. R.C. Reed et al., The Minerals, Metals and Materials Society, Warrendale, PA, 2008, p.109.

[15] R.A. Hobbs, L. Zhang, C.M.F. Rae and S. Tin, Met. Mater. Trans. 39A (2008) p.1014.

[16] W.C. Oliver and G.M. Phar, J. Mater. Res., 7 (1992) p.1564.

[17] K. Durst, M. Göken and H. Vehoff, J. Mater. Res., 19, 1 (2004) p.85.

[18] H.-A. Kuhn, H. Biermann, T. Ungár and H. Mughrabi, Acta Metall. Mater. 39 (1991), p. 2783.

[19] S. Neumeier, J. Ang, R.A. Hobbs, C.M.F. Rae and H.J. Stone, submitted to Materials Science Forum

[20] F. Pyczak, S. Neumeier and M. Göken, Mat. Sci. Eng. A,527, 29-30 (2010) p.7939

[21] M. Göken and M. Kempf, Acta Mat. 47, 3 (1999) p.1043.

[22] L. Müller, U. Glatzel and M. Feller-Kniepmeier, Acta Metal. Mater., 40, 6 (1992) p.1321.

[23] Y. Mishima, S. Ochiai, N. Hamao, M. Yodogawa and T. Suzuki, Trans. Jpn. Inst. Met. 27 (1986) p.656.

[24] L.A. Gypen and A. Deruyttere, J. Mater. Sc., 12 (1977) p.1028.

[25] H.A. Roth, C.L. Davis and R.C. Thomson, Met. Mat. Trans. 28A (1997) p.1329.

[26] F. Diologent and P. Caron, Mat. Sc. Engin. A 385 (2004) p.245.

[27] Y. Mishima, S. Ochiai, M. Yodogawa and T. Suzuki, Trans. Jpn. Inst. Met. 27 (1986) p.41.

Table 1: Nominal composition in wt% (at. %) of the four experimental alloys investigated in this work.

Alloy	Al	Ti	Cr	Co	Mo	Ta	Re	Ru	Ni
Alloy ReRu	4.9 (10.4)	3.9 (4.7)	8.2 (9.1)	4.1 (4.0)	2.5 (1.5)	1.6 (0.5)	3.0 (0.9)	3.0 (1.7)	68.8 (67.2)
Alloy Re	4.9 (10.3)	3.9 (4.6)	8.2 (8.9)	4.1 (3.9)	2.5 (1.5)	1.6 (0.5)	3.0 (0.9)	0.0	71.8 (70.0)
Alloy Ru	4.9 (10.2)	3.9 (4.6)	8.2 (8.9)	4.1 (3.9)	2.5 (1.5)	1.6 (0.5)	0.0	3.0 (1.7)	71.8 (68.8)
Alloy 0	4.9 (10.1)	3.9 (4.5)	8.2 (8.8)	4.1 (3.9)	2.5 (1.5)	1.6 (0.5)	0.0	0.0	74.8 (70.8)

Fig. 1: Exemplary AFM images of a) Alloy Re showing several fields of indents in the γ and γ' phase using a maximum load P_{max} of 250 µN, 500 µN and 1000 µN respectively, b) Alloy Re with secondary γ' precipitates in the γ matrix due to an incomplete heat treatment and c) Alloy 0, d) Alloy Re, e)Alloy Ru and f) Alloy ReRu with nanoindents which were performed at a load P_{max} of 250 µN.

Fig. 2: Load-displacement curves of the γ matrix phase of two different samples of Alloy Re. The different microstructures, with seconday γ' precipitates (Fig.1b) and without seconday γ' precipitates (Fig.1d), were obtained through different heat treatments.

Fig. 3: Two exemplary load-displacement curves each of the γ' precipitate phase and the γ matrix phase and a load-displacement curve which was derived by initial indentation of the γ matrix with a subsequent penetration of a γ' precipitate.

Fig. 4: EPMA mapping of Re in a) the as-cast state and b) after solutioning at 1305°C for 48 hours in Alloy ReRu.

Fig. 5: Hardness of the γ' precipitates and γ matrix of all experimental alloys at a maximum applied force of 250 µN.

Fig. 6: Partitioning coefficient $k_i^{\gamma'/\gamma}$ of the alloying elements in the experimental alloys under investigation.

Fig. 7: X-ray diffraction profile of a) Alloy 0 and b) Alloy Ru at room temperature (dots). The peaks were fitted with Pseudo-Voigt-functions to deconvolute the measured (002) peak into the subpeaks of the γ matrix and γ' precipitates (dashed line).

Fig. 8: Influence of the sum of the atomic concentrations c_i of elements i = Mo, Re and Ru in the γ matrix and γ' precipitates on the hardness of the γ and γ' phase in all experimental alloys. The concentration of the elements in the γ and γ' phase was measured by TEM-EDS.

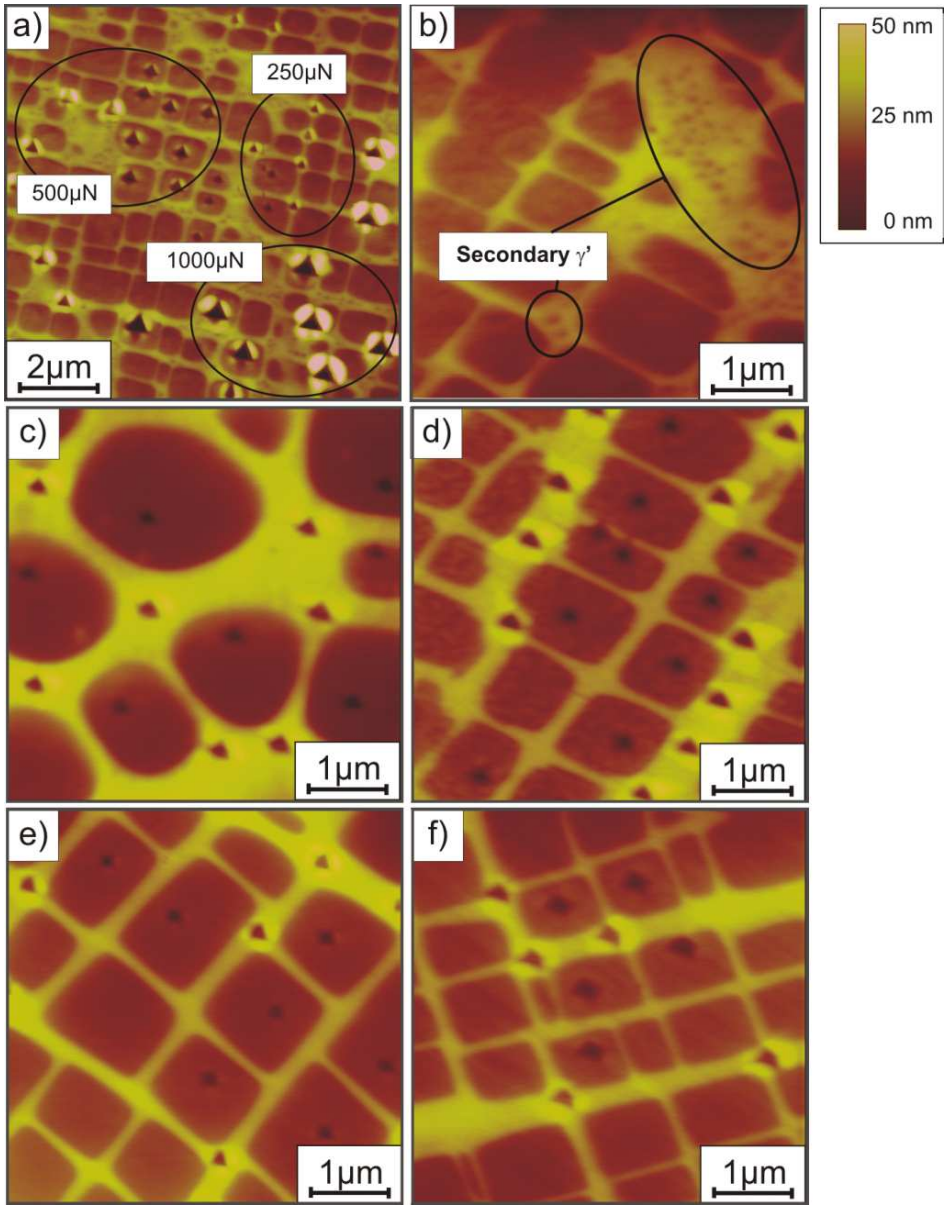

Fig. 1: Exemplary AFM images of a) Alloy Re showing several fields of indents in the γ and γ' phase using a maximum load Pmax of 250 μN, 500 μN and 1000 μN respectively, b) Alloy Re with secondary γ' precipitates in the γ matrix due to an incomplete heat treatment and c) Alloy 0, d) Alloy Re, e)Alloy Ru and f) Alloy ReRu with nanoindents which were performed at a load Pmax of 250 μN.
86x110mm (300 x 300 DPI)

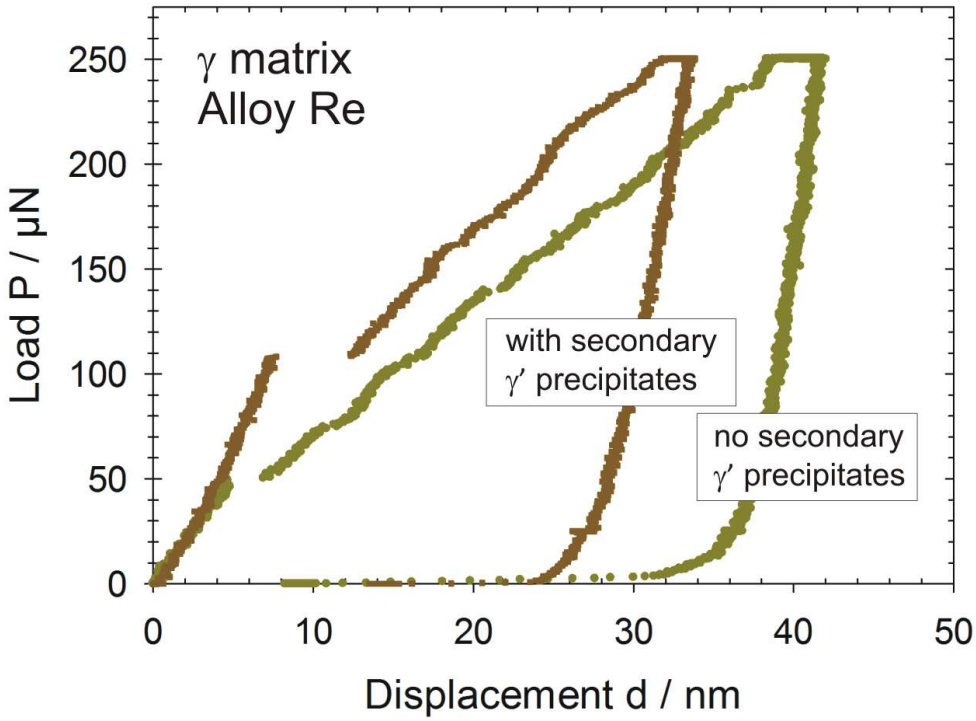

Fig. 2: Load-displacement curves of the γ matrix phase of two different samples of Alloy Re. The different microstructures, with seconday γ' precipitates (Fig.1b) and without seconday γ' precipitates (Fig.1d), were obtained through different heat treatments.

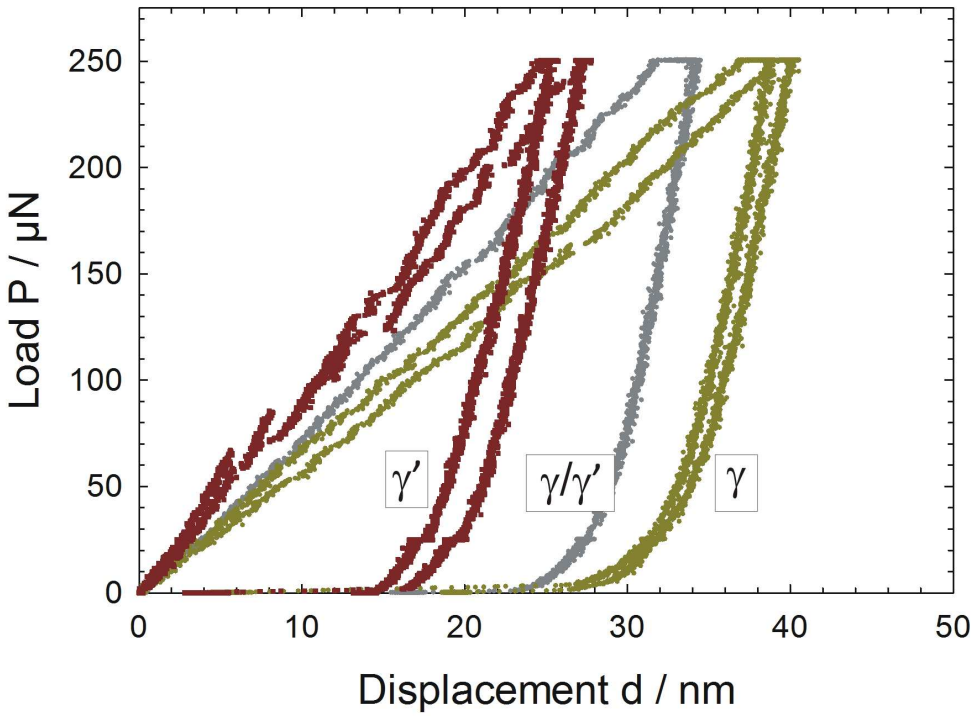

Fig. 3: Two exemplary load-displacement curves each of the γ' precipitate phase and the γ matrix phase and a load-displacement curve which was derived by initial indentation of the γ matrix with a subsequent penetration of a γ' precipitate.

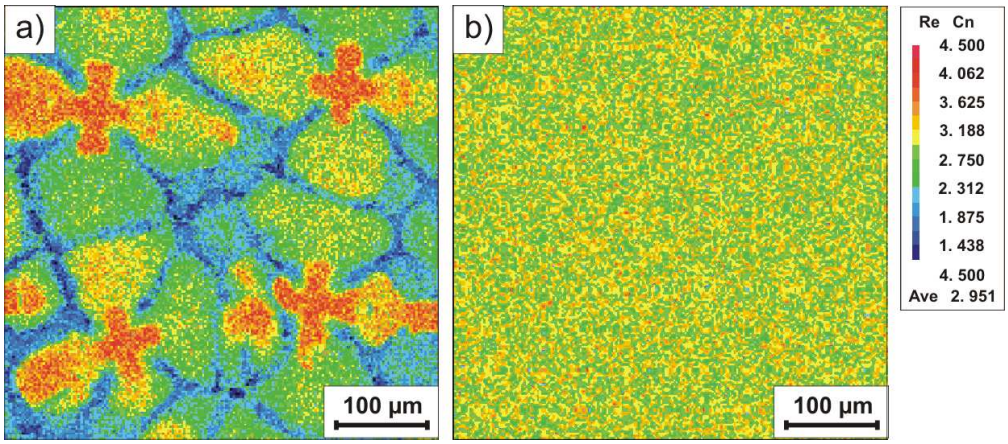

Fig. 4: EPMA mapping of Re in a) the as-cast state and b) after solutioning at 1305°C for 48 hours in Alloy ReRu.

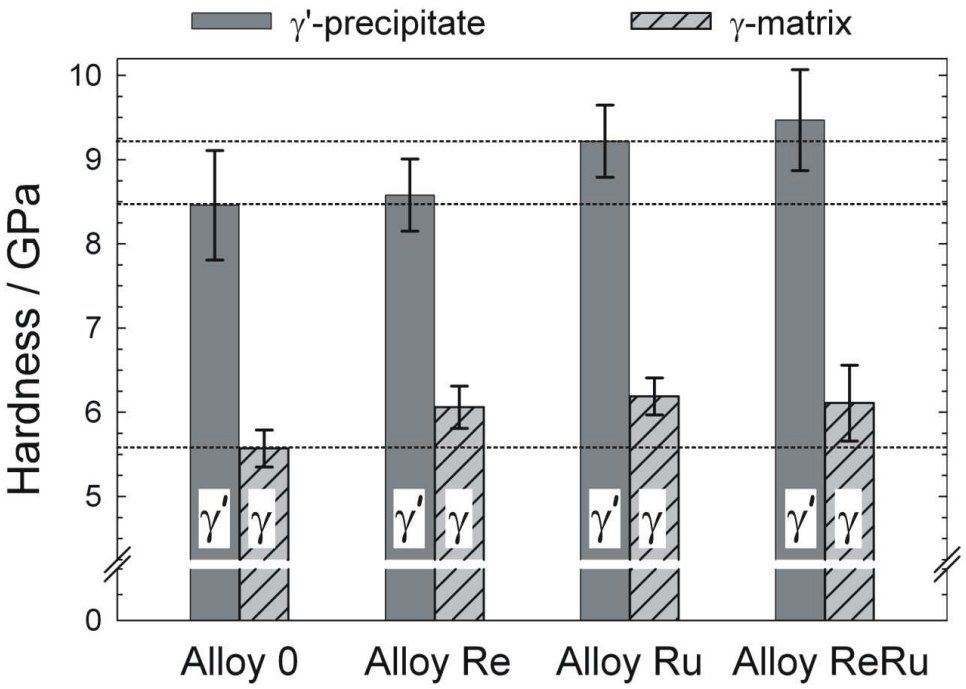

Fig. 5: Hardness of the γ' precipitates and γ matrix of all experimental alloys at a maximum applied force of 250 µN.

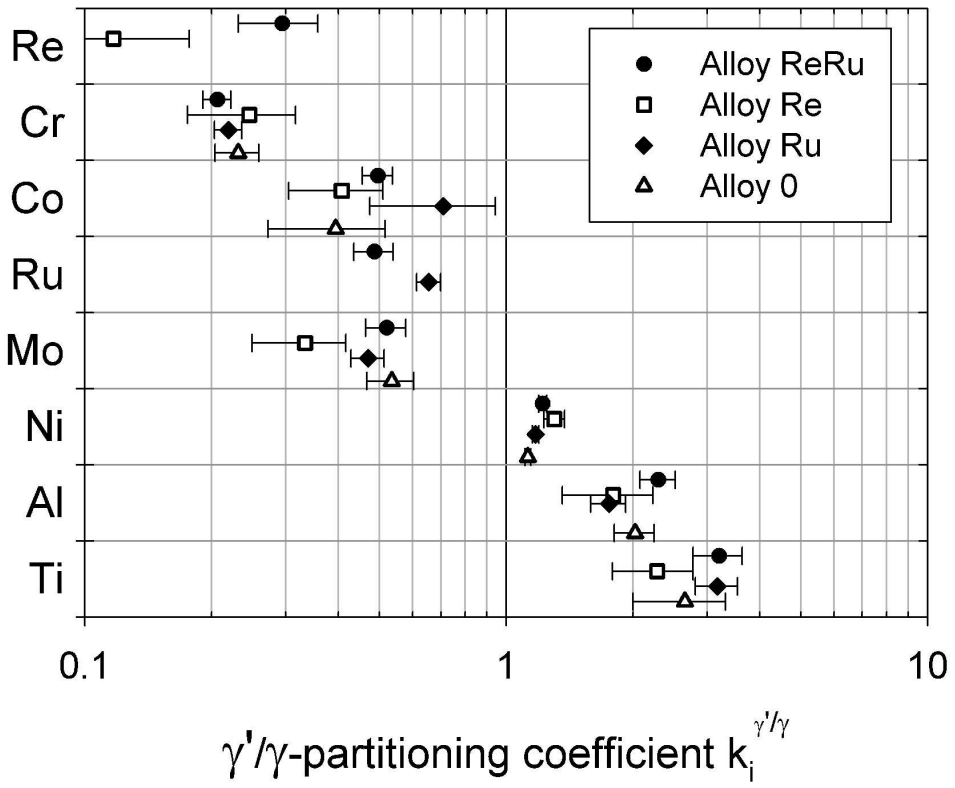

Fig. 6: Partitioning coefficient ki γ'/γ of the alloying elements in the experimental alloys under investigation.

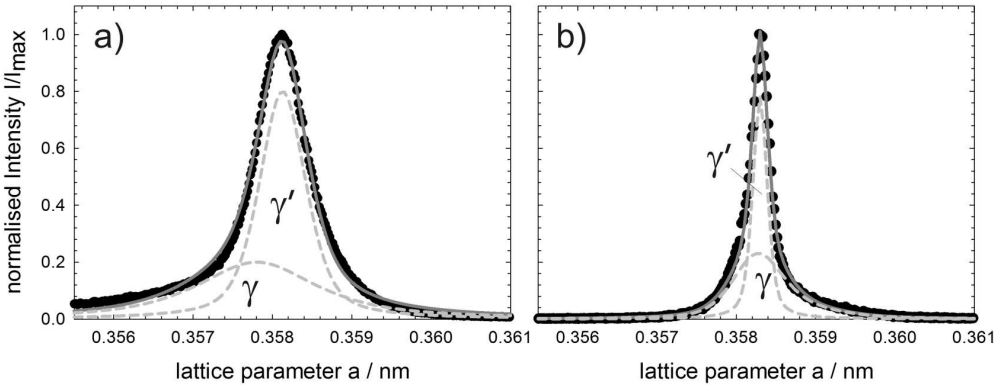

Fig. 7: X-ray diffraction profile of a) Alloy 0 and b) Alloy Ru at room temperature (dots). The peaks were fitted with Pseudo-Voigt-functions to deconvolute the measured (002) peak into the subpeaks of the γ matrix and γ' precipitates (dashed line).

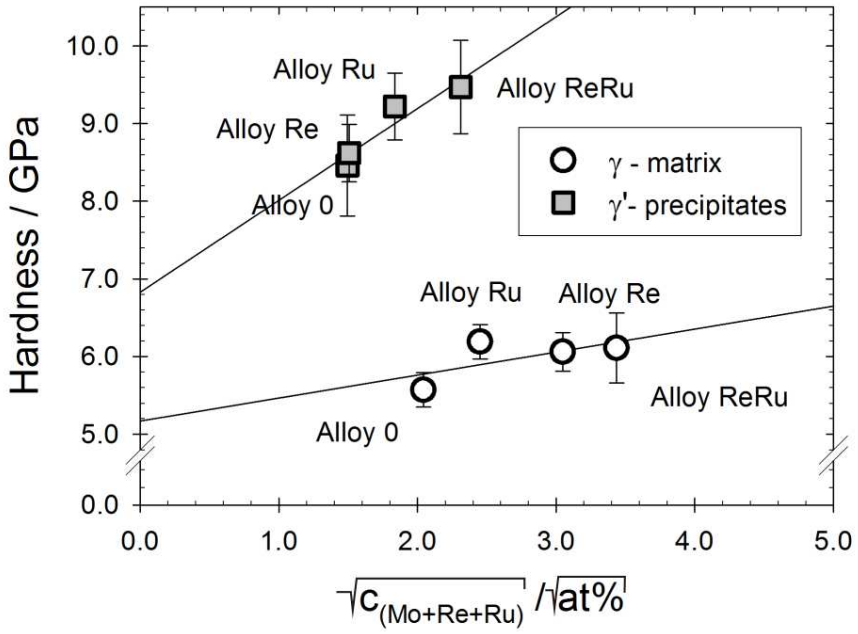

Fig. 8: Influence of the sum of the atomic concentrations ci of elements i = Mo, Re and Ru in the γ matrix and γ' precipitates on the hardness of the γ and γ' phase in all experimental alloys. The concentration of the elements in the γ and γ' phase was measured by TEM-EDS.
90x63mm (300 x 300 DPI)